

NEUROSCIENCE FOREFRONT REVIEW

NEW USES OF LFPs: PATHWAY-SPECIFIC THREADS OBTAINED THROUGH SPATIAL DISCRIMINATION

O. HERRERAS,^{a*} J. MAKAROVA^a AND V. A. MAKAROV^b

^a Department of Systems Neuroscience, Cajal Institute, CSIC, Avenida Doctor Arce 37, Madrid 28002, Spain

^b Department of Applied Mathematics, School of Mathematics, University Complutense of Madrid, Plaza de Ciencias 3, Ciudad Universitaria, Madrid 28040, Spain

Abstract—Local field potentials (LFPs) reflect the coordinated firing of functional neural assemblies during information coding and transfer across neural networks. As such, it was proposed that the extraordinary variety of cytoarchitectonic elements in the brain is responsible for the wide range of amplitudes and for the coverage of field potentials, which in most cases receive contributions from multiple pathways and populations. The influence of spatial factors overrides the bold interpretations of customary measurements, such as the amplitude and polarity, to the point that their cellular interpretation is one of the hardest tasks in Neurophysiology. Temporal patterns and frequency bands are not exclusive to pathways but rather, the spatial configuration of the voltage gradients created by each pathway is highly specific and may be used advantageously. Recent technical and analytical advances now make it possible to separate and then reconstruct activity for specific pathways. In this review, we discuss how spatial features specific to cells and populations define the amplitude and extension of LFPs, why they become virtually indecipherable when several pathways are co-activated, and then we present the recent advances regarding their disentanglement using spatial discrimination techniques. The pathway-specific threads of LFPs have a simple cellular interpretation, and the temporal fluctuations obtained can be applied to a variety of new experimental objectives and improve existing approaches. Among others, they facilitate the parallel readout of activity in several populations over multiple time scales correlating them with behavior. Also, they access information contained in irregular fluctuations, facilitating the testing of ongoing plasticity. In addition, they open the way to unravel the synaptic nature of rhythmic oscillations, as well as the dynamic relationships between multiple oscillatory activities. The challenge of understanding which waves belong

to which populations, and the pathways that provoke them, may soon be overcome. © 2015 IBRO. Published by Elsevier Ltd. All rights reserved.

Key words: local field potentials, independent component analysis, neural source localization, network oscillations, population activity, spontaneous activity.

Contents	
Introduction: there is no time without space	487
The spatial problem	487
Recent technological advances have opened new experimental possibilities	488
LFP generators: a local window to distant activity	489
The spatial nature of LFPs	489
LFP basics: the relevance of geometry	489
Subcellular location and chemical nature of the inputs	491
A note on temporal factors and spatiotemporal intermodulation	491
From spikes to LFPs: pathway-specific activity has an anatomically defined and characteristic spatial profile	492
Mixing and de-mixing LFP sources	492
A cocktail party problem	492
Understanding instantaneous spatial profiles	492
Anatomical correlates of spatial profiles	493
Sampling three-dimensional voltage shells with linear probes	493
Some weaknesses of ICA of LFPs: Intracellular blending of currents	495
Limitations of ICA for spatially shifting LFPs and hypersynchronous events	495
Applications of pathway-specific LFP generators	496
Network dynamics: continuous parallel readouts of several population outputs	496
Access to information contained in irregular fluctuations	496
Grouping LFP events that originate in a common population	496
Assessing ongoing plasticity	496
Long-term effects of pharmacological treatment, genetic differences and pathology	496
Exploring population activities over different time scales	497
Active networks in different brain states	497
Cellular and biophysical mechanisms	498
Identifying the true polarity and amplitude of pathway-specific postsynaptic currents	498
LFP polarity does not identify excitation or inhibition	498
Discriminating local and volume-conducted contributions	498
Identifying pre- and postsynaptic units in spike-phase plots	499

*Corresponding author. Tel: +34-915854725; fax: +34-91-5854750. E-mail addresses: herrerass@cajal.csic.es (O. Herreras), makarovaj@cajal.csic.es (J. Makarova), vmakarov@mat.ucm.es (V. A. Makarov).

Abbreviations: AC/DC, alternate current/direct current; CA1–3, cornu ammonis 1–3; CSD, current source density; DG, dentate gyrus; f-EPSP, field excitatory postsynaptic potential; GABA, gamma aminobutyric acid; ICA, independent component analysis; LFP, local field potential; V_o , extracellular voltage.

Identifying the topology of connections through spatial modules of coherent activity	499
Technical aspects of ICA usage on LFPs:	
Hints and workarounds	499
Some general considerations	499
Preprocessing: goods and bads	499
The removal of ultraslow (DC-coupled) potentials	499
Filtering	499
The reduction in dimensionality	500
Hints: maximizing the contribution of the source of interest	500
Repeated analyses of the same LFP epochs using different groups of channels	500
Optimizing the electrode placement	500
Priming the pathway of interest	500
Concluding remarks: a new era for LFPs	500
Acknowledgements	501
References	501
Appendix A. Supplementary data	503

INTRODUCTION: THERE IS NO TIME WITHOUT SPACE

Information processing and transfer between higher brain centers is largely based on the coordinated firing of functional groups of neurons or assemblies. At the circuit level, the synchronous firing of neuron assemblies promotes the addition of synaptic currents in the volume of tissue surrounding the target neurons. These currents may give rise to measurable extracellular field potentials, providing a link between neural activity and behavior (Buzsáki et al., 1983; Jacobs and Kahana, 2010; Womelsdorf et al., 2014).

Non-invasive EEG recordings reflect the coherent activity over large cortical and sub-cortical regions, and they are widely employed in medical applications (Cooper et al., 1965; Lopes da Silva and Van Rotterdam, 1982; Niedermeyer, 2003). On the mesoscopic scale, the activity of individual neuronal circuits and pathways can be picked up by intracranial electrodes as local field potentials (LFPs). The ease of recording explains why LFPs were one of the first measures of neural activity, and they have helped establish the role of different brain regions, circuits and local networks in specific behavioral manifestations and cognitive tasks, including the phases of the sleep–wake cycle, sensory processing, sensory–motor integration, intention and decision making among others (Dement and Kleitman, 1957; Vanderwolf, 1969; Gray et al., 1989; Destexhe et al., 1999; Pesaran et al., 2002; Seydhosseini et al., 2015; Waldert et al., 2015). The use of LFPs is less extended due to intrinsic difficulties of their interpretation, as we will discuss below. Nevertheless, LFPs contain a surprisingly large amount of information regarding the functioning of neural circuits, information that remains largely unexploited (Eckhorn, 1994; Bullock, 1997; Goldwyn et al., 2014).

The spatial problem

The richness of the temporal dynamics is the most valued information contained in LFPs and EEGs. However, electrodes pick up activities originating from multiple

sites that make extremely difficult to know which waves belong to which populations and the pathways that provoke them (Fig. 1). Localization of the sources of neural activity is a classical problem in Neurophysiology, requiring spatial treatment of the signals. While the long distances from their sources fostered theoretical developments and the use of specific spatial techniques for EEGs (Nunez and Srinivasan, 2006), this has not been considered so necessary for LFPs. Nevertheless, the proximity of LFP recordings to cell sources makes them even more sensitive to local geometrical factors. Such factors may lead to counterintuitive deductions, whereby major anatomical pathways may render no contribution to LFPs while a minor pathway may originate large LFPs. Moreover, no activity will be reflected in the EEG if there isn't a matching intracranial LFP, although the respective temporal features may differ considerably due to the different spatial scales involved (DeLucchi et al., 1962). Accordingly, to properly understand EEGs it is necessary to fully consider the spatial features of individual intracranial sources and their blending at a distance (volume conduction).

Many studies of LFPs have simply avoided the spatial problem, while others circumvent this and used averaging or temporal waypoints to discard activity unrelated to the events of interest (e.g., evoked potentials, event-related potentials). Conventional statistical tools that are based on time-series analyses (wavelet, coherence, partial

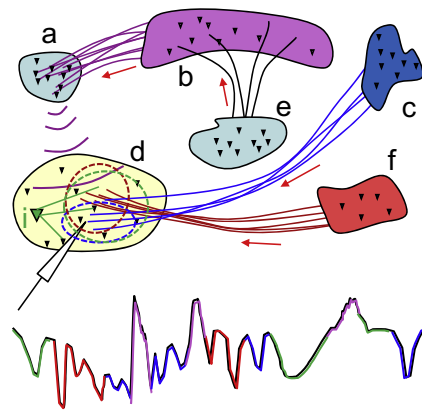


Fig. 1. (A) Local and remote contributions to LFPs. Neuronal populations receive inputs and also project to other populations. Though LFPs may be physically generated by one population, they reflect the output activity of other populations. Therefore the dynamics of several populations is mixed in LFP recordings. In the scheme, the structures (c) and (f) send spikes (arrows) to population (d), producing synaptic currents and LFPs there (local sources from remote populations). Population (d) also receives spikes from local interneuron population (i), which also adds synaptic currents (local source from local population). In addition, although population (a) is not connected to (d), its own synaptic currents build up field potentials that arrive to (d) through the volume (remote sources). Note that these actually represent the output activity from spikes in a third-party population located somewhere else (b). The lower trace is an imaginary single-point recording illustrating the multifold composition of waves recorded within population (d). The respective origins are indistinguishable but each convergent input produces characteristic voltage gradients (ovals) within (d) that can be picked up with multi-electrode arrays, then serving to separate the inputs and reveal the pathway-specific dynamics.

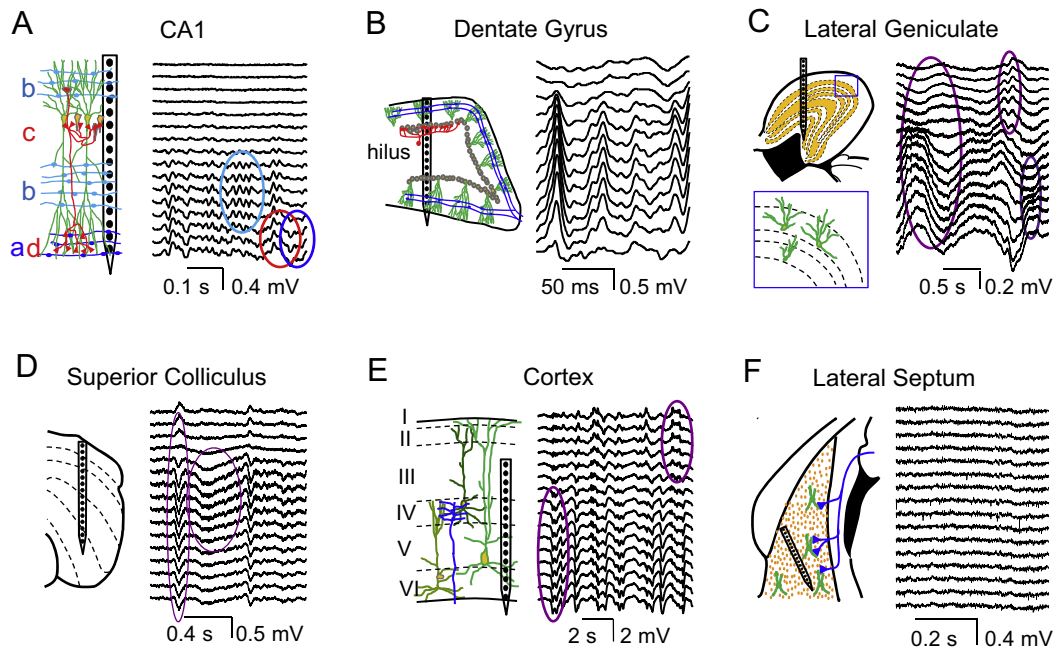


Fig. 2. Cytoarchitectonic determinants of LFP magnitude. In many brain structures, linear recordings allow the discernment of multiple “bands” (ovals in the right side panels) where LFP activity has similar features, each reflecting activation by different anatomical pathways converging on the recorded structure. However, the correspondence of synaptic territories and LFP “bands” is however no intuitive due to the varying combination of cytoarchitectonic factors (left panels): only some cell types and afferent pathways contribute to LFPs in each structure. Sample excitatory and inhibitory pathways and the corresponding LFP bands are drawn in blue and red, respectively (those in purple have unknown origin). (A) Hippocampal CA1: the excitatory Temporo-amonic input (a) to cells arranged in palisade builds LFPs matching the synaptic territory (blue oval). However, the wider distribution of excitatory Schaffer-Commissural inputs (b) builds LFPs in the apical (light blue oval) but not in the basal dendritic arbor. Inhibitory inputs contribute negligibly in the soma region (c), but significantly in other strata (d). (B) Dentate Gyrus: this structure displays giant positive LFPs with a contribution from both dendritic excitatory and somatic inhibitory inputs to granule cells, although its folded architecture makes them reach maximal amplitude in the hilus, far from the synaptic territories. (C) Lateral geniculate nucleus: multipolar tufted neurons with an orthogonal dendritic arrangement with respect to the folded laminae generate multiple bands of distinct LFP activity. The sample LFPs were reconstructed after removal of the distant contributions using analytical techniques. (D) The superior colliculus also shows lamina-specific LFPs. (E) Cortex: this structure contains several neuron subtypes with a morphology suitable to contribute to LFPs. (F) Lateral Septum: small disordered neurons build tiny LFPs even from inputs known to raise LFPs in other structures (e.g. those originating in CA3). All recordings are from anesthetized rats, except (C) (awaken monkey). Length covered: (A) 750 μm ; (B) 1.2 mm; (C) 3.1 mm; (D–F) 1.5 mm. (A–C, F) modified from Benito et al. (2014), Fernández-Ruiz et al. (2013), Makarova et al. (2014), and Martín-Vázquez et al. (2015), respectively.

directed coherence and decomposition into frequency bands) are either inadequate to separate the sources within a volume, or they severely limit access to the continuous flow of information contained in them (Fernández-Ruiz and Herreras, 2013; Pascual-Marqui et al., 2014). Indeed, the cellular interpretation of LFPs has relied mostly on correlations with contingent events, such as e.g., multiunit activity (Buzsáki et al., 1983; Chrobak and Buzsáki, 1998; Fuentealba et al., 2005; Kreiman et al., 2006; Liu and Newsome, 2006; Belitski et al., 2008; Rasch et al., 2009; Beltramo et al., 2013). However, multiunit activity is highly susceptible to subsidiary correlations in complex networks, such as those emanating from the correlated firing of multiple neuron types in parallel circuits. Besides, the fact that spikes represent the output of neurons nearby the electrode is frequently overlooked, while LFPs recorded by the same electrode reflect synaptic currents (i.e., the spike activity of other populations).

Recent technological advances have opened new experimental possibilities

Modern high-density multielectrode arrays and amplifiers connected to a laptop have permitted the simultaneous

sampling of LFPs at hundreds of points. This enables more details of LFPs to be accessed over multiple spatio-temporal scales. Coping with fast fluctuations and submillimeter spatial resolution is no longer a technical problem, and the cellular explanation of LFPs and EEG based on direct measurement of microscopic sources may be just around the corner. Paradoxically the time may not quite be right. Improvements in multirecordings have also brought to light the aforementioned spatial problem that makes the cellular interpretation of raw LFPs virtually undecipherable. It is now easy to appreciate rolling bouts of coherent LFP activity that span different groups of electrodes on a computer screen, in most cases overlapping (Fig. 2). This is because multiple pathways generate concurrent currents and their electric fields expand in space and mix (Video 1). Indeed, to describe the information flow in a brain region quantitatively from LFPs, the activity elicited by each afferent population requires the pathway-specific threads to be reliably separated.

Since temporal patterns of activation are not population exclusive (Bullock et al., 2003), separation can only be achieved through disclosing the respective voltage shells produced by the postsynaptic currents that

each pathway raises in the volume. These currents are related to unique pathway-specific features, such as the location and geometry of the synaptic territory, and they can be matched to anatomy. On the one hand, recordings should simultaneously span a fraction of the volume sufficiently large as to be able to reconstruct the spatial distribution of the field potentials. On the other hand, the analytical techniques should be able to detect the sites where each pathway creates the strongest voltage gradients, efficiently separating them to remove mutual interference. A promising approach for this is based on techniques that allow activities to be discriminated that are coherent within defined spatial domains, such as the independent component analysis (ICA: Comon, 1994), a subclass of modern “blind” algorithms (Hyvärinen et al., 2001). This approach has already become customary in the analysis of surface EEG and fMRI data (Stone et al., 2002; Onton et al., 2006), and it has also been successfully applied to study other brain phenomena requiring spatial discrimination, e.g., sorting spikes from different neurons or disclosing the contributions to event-related potentials (Rauch et al., 2008; Turi et al., 2012). Importantly, this approach has also proved to be useful to efficiently preserve the spatial and temporal information in components disentangled from multisite LFPs (Makarov et al., 2010; Makarova et al., 2011; de Cheveigné et al., 2013; Benito et al., 2014; Schomburg et al., 2014).

LFP generators: a local window to distant activity

The ICA approach involves the use of multiple LFP signals recorded simultaneously over a brain area that sample the three-dimensional voltage shell produced there by local and remote current sources, and it returns a series of components that each describe a virtual estimate of the location and activity of one of them. These correspond to readouts of the postsynaptic activity elicited by one afferent population on another, referred to as LFP generators (Makarov et al., 2010). Therefore, once a set of LFP generators has been assigned to a structure, the activity of several afferent populations identified can be followed from a distance, i.e., no direct recording in those regions is generally required (Fig. 1). Reliable and consistent sets of LFP generators have been found in several structures and although their identification may require multiple checks, they constitute a catalog that can be used to study network dynamics with unprecedented quantitative power and temporal resolution.

This review focuses on the aspects that help us understand how sources mix in the volume and their disentanglement through the analysis of experimental data. We first recall a few basic concepts relating unitary currents to pathway-specific and multisource LFPs and present the recent progress on the use, interpretation and foreseen limitations of the ICA for the spatial discrimination of the mixed sources (see the section on ‘The spatial nature of LFPs’). We then expose some of the new applications to the study of cell and network activity (see the section on ‘Applications of pathway-specific LFP generators’), and finally we lay

some practical hints to optimize separation (see the section on ‘Technical aspects of ICA usage on LFPs: Hints and workarounds’), for which we provide prospective users free access to our software (LFP-sources®) that contains several ICA algorithms along with pre- and post-processing tools (<http://www.mat.ucm.es/~vmakarov/downloads.php>).

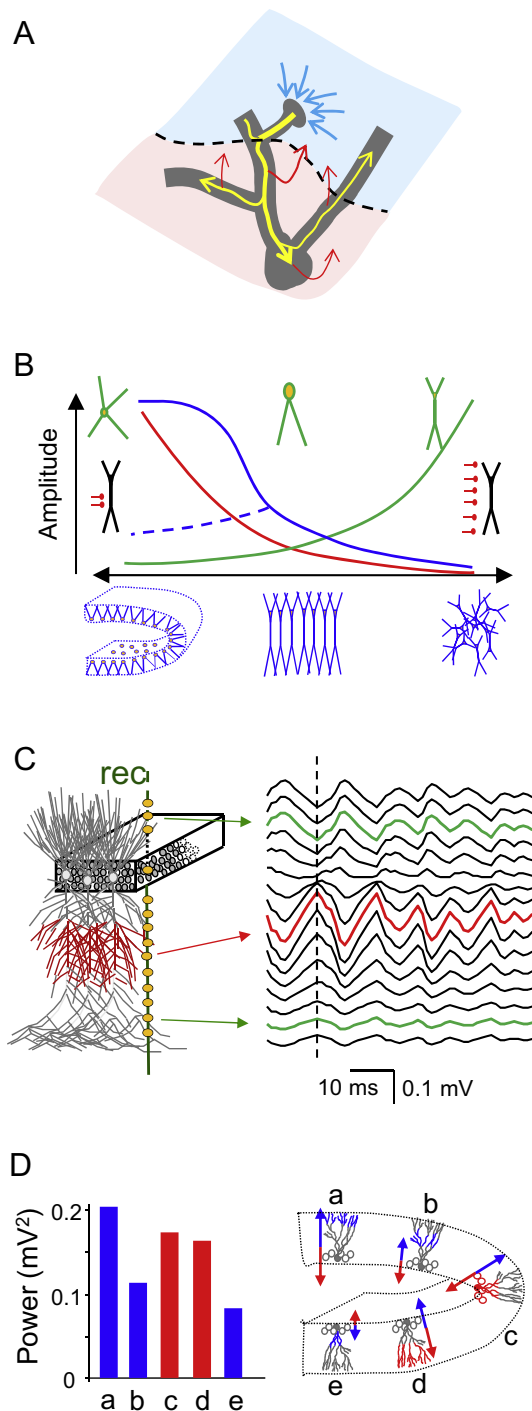
THE SPATIAL NATURE OF LFPs

The pioneers in the study of LFPs identified the extraordinary complexity of neural current sources as the main obstacle for their exploitation, and flagged cytoarchitecture as the limiting factor (Lorente de Nó, 1947; Woodbury, 1960; Rall and Shepherd, 1968). Classic theoretical studies anticipated that the amplitude of LFPs depends on cell morphology (axial is more favorable than radial), the distribution of inputs (clustered is better than scattered) and population arrangement (orderly populations render larger LFPs than glomerular ones: Fig. 3B). As a rule of thumb only combinations of inputs and target populations that establish sufficient spatial segregation of inward and outward currents in the extracellular space raise measurable LFPs. Thus, the LFP magnitude depends not as much on the strength or the chemical nature of the inputs as in the way individual cells and the neuronal populations distribute these currents in the volume. Recent empirical studies using pathway-specific LFPs indeed confirmed that not all anatomical pathways contribute to LFPs (Benito et al., 2014) nor does a given population produce LFPs in all its downstream targets (Martín-Vázquez et al., 2015). For an extensive review of theoretical and formal aspects we refer the readers to comprehensive monographs (Lorente de Nó, 1947; Rall and Shepherd, 1968; Elul, 1971; Lopes da Silva and Van Rotterdam, 1982; Gloor, 1985; Nunez and Srinivasan, 2006), and to additional more recent texts that discuss some specific issues regarding LFPs (López-Aguado et al., 2002; Bedard et al., 2004; Lindén et al., 2011; Buzsáki et al., 2012; Schomburg et al., 2012; ęski et al., 2013; Martín-Vázquez et al., 2013, 2015; Fernández-Ruiz and Herreras, 2013; Reimann et al., 2013; Petersen et al., 2014).

LFP basics: the relevance of geometry

If we graphically portray the basic concepts of LFPs (Figs. 3 and 4), some of them that will repeatedly be considered to evaluate the performance of the ICA on LFPs can be listed:

- (1) LFPs are produced by neuron populations that receive synaptic input and thus, they echo the spike output of *upstream* populations (the targeted neurons that generate the LFP may fire or not). Fig. 1 illustrates the possible origins of activities blended in LFPs. On the one side, the local sources are those generated by synaptic currents of neurons near the electrodes and in turn these can be elicited by local or remote populations of origin, such as nearby interneurons or projection cells from distant



regions, respectively (e.g., local population *i* and distant populations *c* and *f* projecting to population *d*). In addition, other volume-conducted contributions may arrive from remote locations (e.g., from population *a*). However, it is important to note that remote contributions do not reflect the output activity of the population from which they originate but rather, that of third party populations that project there (population *b*). Indeed, remote contributions dominate in regions whose local generators are weak.

(2) At any instant a synaptic input produces a balanced amount of inward/outward transmembrane current over the entire anatomy of individual neurons. Although active currents occur at synaptic knobs, they return to the extracellular space after traveling varying distances through complex arborized morphologies (Fig. 3A). These define where the currents are re-injected and whether they will add or subtract to others from the same or other neurons, which has two immediate implications: (a) the cytoarchitecture of the target population and the location of the synaptic territory are both limiting factors for the buildup of voltage shells by a given pathway (Fig. 3B); for instance, a suitable population architecture may render no LFPs if the synaptic territories of the inputs are scattered all over the somatodendritic membranes of the target cells, leading to a massive cancelation of currents in the vicinity of individual cells. (b) LFP polarity does not reflect the excitatory/inhibitory nature of the synaptic currents as the sign may change over the length of the neuronal structure. Fig. 3C illustrates this concept with a rhythmic input to an orderly planar population where one may appreciate that similar LFPs would be obtained whether the input is excitatory or inhibitory (this is further complicated by other sub and supracellular factors as discussed below: see Fernández-Ruiz and Herreras, 2013; Martín-Vázquez et al., 2015, for an in-depth analysis).

Fig. 3. Factors and features relevant to LFP buildup. (A) LFP buildup requires charge separation in the extracellular space that is provided by inward (blue) and outward currents (red) during synaptic activation. The geometry of neurons defines the intracellular current path (yellow arrows) and hence, the sites where the current returns. In the outside, the currents have a chance to add or subtract to those from other neurons and raise extracellular dipoles. Blue and pink backgrounds represent negative and positive field potential areas. (B) Schematic representation of the impact that structural factors have on LFP amplitude. The three main anatomical determinants are depicted in green, red and blue respectively; cell morphology (from left to right: radial, tufted and axial); input distribution (clustered and scattered); and population architecture (folded, planar and glomerular). Folded structures build larger LFPs on the inner side and smaller on the outer side (dashed limb). (C) Polarity does not reflect the chemical nature of LFPs. Synchronous synaptic input to homologous regions of neurons in a population (e.g., to dendrites in red) produces field potentials of opposite polarity in sites nearby due to the spatial segregation of inward and outward currents. This is true whether the synaptic input is excitatory or inhibitory. (D) Subcellular location of the inputs. Estimations are from synthetic LFPs using a realistic model of the folded Dentate Gyrus. The amplitude of LFPs is larger for inputs at cell edges (somatic or dendritic) than in the middle portions, whether excitatory (blue) or inhibitory (red). Blue and red cell portions indicate synaptic territories of different anatomical pathways to hippocampal granule cells: (a, e) lateral and medial perforant paths, basket cell somatic inhibition, dendritic inhibition, and proximal commissural input. The latter two are not detected in experiments. The double-headed arrows indicate the direction and polarity of the generated field potential dipoles, all of which are positive between granule cell layers except that for dendritic inhibition. (C and D) From Martín-Vázquez et al. (2013) and Fernández-Ruiz and Herreras (2013), respectively.

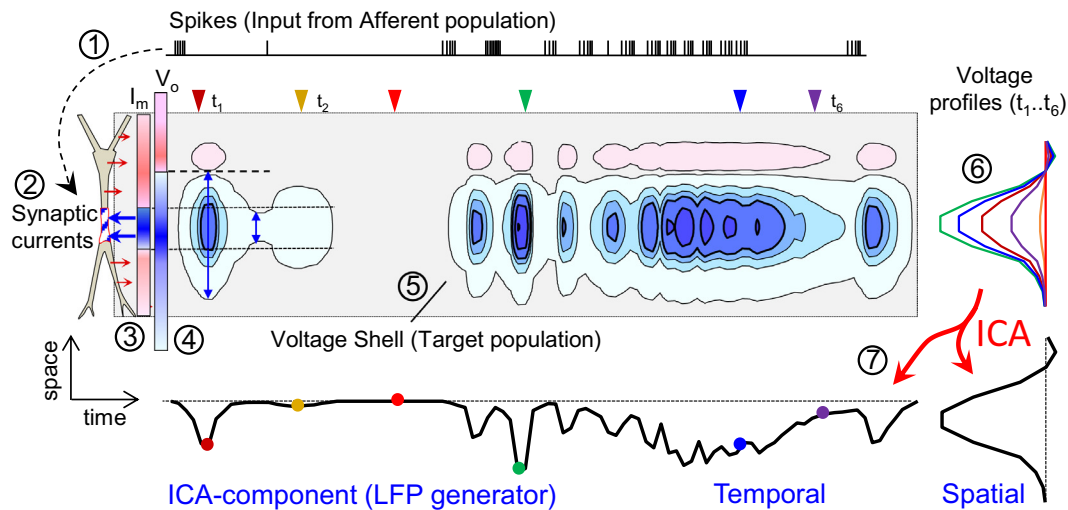


Fig. 4. From spikes to LFPs. A train of afferent spikes (1) emitted by an upstream excitatory population generates synaptic currents (2) in the apical tree of a target population (cell dummy). (3) The postsynaptic cells produce inward currents in the synaptic zone (blue arrows) that loop outward through adjacent membranes (red arrows), raising sinks and sources in the extracellular space (quantified as color density in the I_m bar). (4) Jointly they produce a dipolar field potential profile (V_o) [represented by isopotential contour plots in blue (negative) and red (positive) tones]. V_o is decreasingly negative from the synaptic zone and extends beyond the physical sources. The I_m and V_o polarity reversal may not coincide as this depends on the cell's geometry, and in the example it reverses in the soma layer (dashed line). (5) The different strength of I_m over time leads to a time-varying voltage shell and the amplitude fluctuations roughly follow the sequence of afferent spikes. Importantly, the amplitude fluctuations are paralleled at all sites, synaptic and non-synaptic zones, together appearing as if the potentials “reach” a different distance (vertical double-headed arrows). (6) This is appreciated in the superposed instantaneous profiles corresponding to instants t_1 – t_6 (triangles) that are spatially proportional. (7) The entire spatiotemporal V_o shell is loaded as a data matrix for the ICA that looks for proportional variations at all electrodes. In the simple case illustrated, only one significant component is returned with a unique spatial distribution. Note that the amplitude of the successive instantaneous profiles equals the varying strength of activation (dots on the black trace) and thus, the temporal dynamics are reconstructed from the normalization factor of the successive profiles.

- (3) Since currents spread in the volume and mix, and in order to correctly assign temporal fluctuations of LFPs (item 1) to anatomical pathways (item 2), an efficient separation of the contributions elicited by different afferent populations is obligatory. Defining the currents produced by a target population (i.e., population-specific LFPs: Gratny et al., 2011) is not sufficient given that several pathways converge on a common target.

Subcellular location and chemical nature of the inputs.

An additional factor modulating the amplitude of LFPs is related to the somatodendritic location of the inputs. In general, those located in the outer segments build larger LFPs than others located in the middle regions due to the stronger dipolar moment of the former (Fig. 3D). Although inhibitory inputs prevail in the soma of many neuron types, so far there is no evidence of a preferred excitatory or inhibitory contribution to LFPs. In some well-explored structures like the hippocampal CA1 region, some powerful excitatory pathways build LFPs of moderate amplitude but others contribute negligibly. Similarly, powerful somatic inhibition has a negligible contribution in this region but a significant influence in the CA3 and the DG (Korovaichuk et al., 2010; Benito et al., 2014; Martín-Vázquez et al., 2015). In addition, excitatory or inhibitory pathways may have a different relative contribution in different behavioral states (Haider et al., 2013). With regard to the amplitude and polarity of LFPs, computational studies indicate that spatial fac-

tors override the chemical nature of the input (Makarova et al., 2011; Fernández-Ruiz et al., 2013).

A note on temporal factors and spatiotemporal intermodulation

There are other factors that are not merely structural that may strongly modulate LFP amplitude, among which the most relevant are the rate and synchronization of the elementary contributions. These are not analyzed in this review (see e.g., Elul, 1971), but both these features maintain a direct relationship to LFP amplitude, albeit with one important exception: when LFPs are recorded in alternate current (AC)-coupled mode. Thus, the higher the mean rate of elementary inputs the more often the slow and direct current (DC)-like potentials build up due to the temporal overlap of elementary currents. Since these are filtered out by AC-coupled recordings, the remaining AC becomes smaller and may even disappear. This is probably why many anatomical pathways apparently contribute negligibly to LFPs, particularly when cells in the origin population fire at high rates.

Spatial factors are of structural origin and hence, their impact on LFP amplitude is stable. One may view their role as a site-specific multiplier of the amplitude set by temporal factors, ranging from zero to one in the different pathways. It is important to understand that the mean relative amplitude of pathway-specific contributions cannot be used to imply different levels of activity in the pathways. However, their relative changes over time can, providing highly valuable information on network dynamics (see below).

From spikes to LFPs: pathway-specific activity has an anatomically defined and characteristic spatial profile

The synaptic currents elicited by each afferent pathway in the target population produce an electrical field that decays over distance. The so-created spatial field potential gradients have a characteristic distribution akin to the depth profiles in standard evoked potentials (Korovaichuk et al., 2010). The cellular basis underlying the post-synaptic convolution of a series of afferent spikes into variations of the extracellular potential (V_o) can be illustrated (Fig. 4), whereby isopotential surfaces adopt a curvilinear concentric configuration reminiscent of Matryoshka dolls. Ideally, linear recording arrays puncture all of these layers, providing characteristic linear sample maps that may be used along with anatomical information to infer the location and features of the current source. In such simple cases, the sum of the currents from many cells may give rise to LFPs in a well-defined laminar profile. However, spatial gradients are not static and rather, they change dynamically over time as a function of the intensity of the current (see Video 1). Importantly, this allows them to reach different distances from the source. As might be expected for static sources, the only feature that remains constant is the proportional value of the electric field in space. Hence, the spatial profile of the resulting field potential at any instant can be normalized to a unique spatial distribution that is characteristic of each synaptic pathway and target region (t_1 – t_6 in Fig. 4). Spatial profiles are easily recognizable and they remain robust across animals as they are derived from stable macroscopic averages of microscopic structural factors. However, their shape is not always intuitive and it must be learned empirically (see below).

Mixing and de-mixing LFP sources

A cocktail party problem. The separation of the sources mixed in LFPs is analogous to the problem of the *cocktail party*: how can one listen to a single

person's voice among so many in a room. If the speaker doesn't move this can be achieved through an ICA that takes up the sounds picked up by several scattered microphones, extracting those that arrive to all of them with a fixed set of proportional values. For the most part, the sources of current in the brain are immobile and hence, each produces fluctuating electrical field with proportional values in space. The problem is then reduced to find and classify the parts of the LFPs that reach the electrodes *with proportional values*.

Understanding instantaneous spatial profiles. The separation of mixed neural sources is better understood if we first describe how they blend into a synthetic LFP, as observed through detailed computer-assisted models of realistic anatomy (Makarov et al., 2010; Makarova et al., 2011; Lindén et al., 2011; Martín-Vázquez et al., 2013, 2015). To this end, it is most convenient to think of the spatiotemporal maps of V_o as a sequence of instantaneous spatial profiles. If we consider a forward solution of LFPs elicited by combining two afferent inputs to the same population (Video 2), when only one pathway is activated, the respective spatiotemporal shell of V_o can be described as a sequence of n instantaneous spatial profiles of identical shape but different amplitude. If two or more pathways are co-activated, the mixed LFPs contain an uneven proportion of each profile at different recording sites and instants, and the collection of the spatial profiles becomes highly heterogeneous. One may imagine the ICA operation as a “sorting” of these instantaneous profiles. Those that are very similar are accrued into one LFP generator that fully matches one or another pathway, while those with a mixed contribution have to be split into adequate proportions. The process is graphically represented in successive steps for a real case of LFP recordings obtained with a linear array placed across hippocampal layers that receive a contribution from what is *a priori* an unknown number of synaptic pathways (Fig. 5). The recordings can be loaded into an input matrix with rotated time and space axes, and the algorithm finds and classifies the most common spatial distributions by

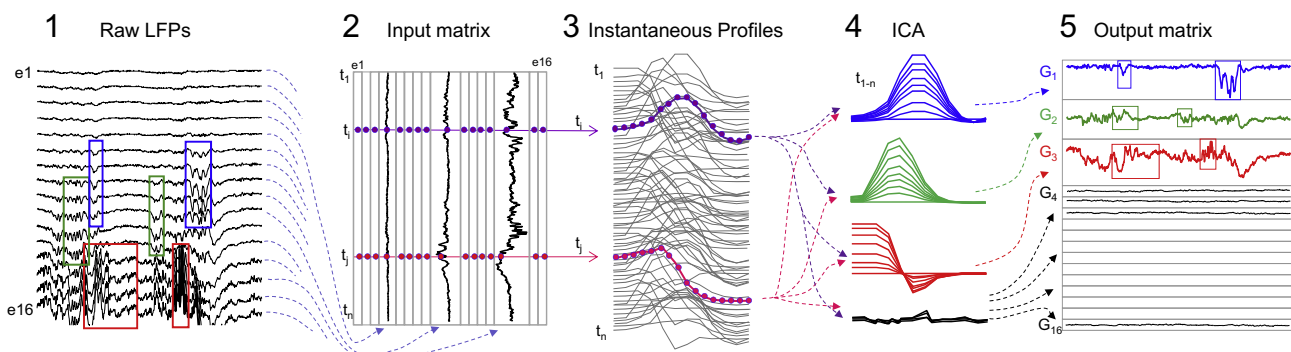


Fig. 5. Disentanglement of pathway-specific LFP generators from multisite linear recordings using independent component analysis (ICA). Hallmarks of this process are depicted in five steps from left to right. Raw LFPs (1) are used to build an input matrix where space and time are rotated (2). Note that the rows in the matrix represent instantaneous field potential profiles (3) whose gradients are created by one or several site-specific currents. These vary over time according to the natural co-activation of converging pathways. (4) The ICA finds a set of proportional values between all sites (i.e.: spatial profiles), each of which corresponds to that created by individual pathways on their target populations. (5) Re-ordering the varying amplitude of each class of profiles (rows in the output matrix) provides a sequence of values that is proportional to the fluctuating strength of each profile over time, i.e.: pathway-specific virtual LFPs.

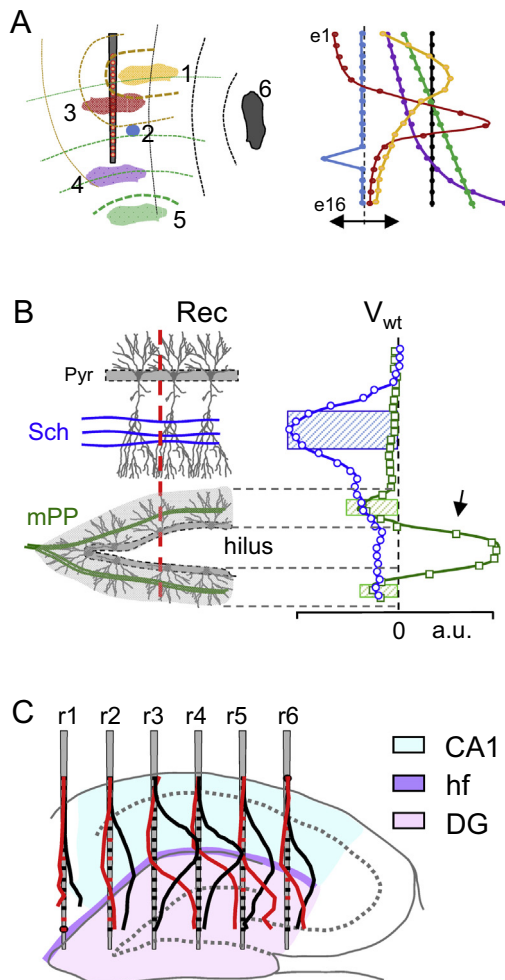


Fig. 6. The spatial distribution of pathway-specific LFPs is stable and hints to the location of the source related to the recordings. (A) Left panel: different sources of current (colored surfaces) located in different positions with respect to the recording array. A linear array “cuts” the respective V_o shells at different angles, and the resultant voltage profile indicates the remote or local position. The profiles to the right correspond to archetypical configurations obtained by applying an ICA to a LFP matrix of 16 linear sites. Local sources yield bell-shaped profiles (1 and 3) with maxima close to the synaptic territory and they may have a polarity reversal if the array crosses a zero surface in the dipolar fields. Exponential-like profiles denote nearby sources above or below the linear array (4). The V_o profiles become monotonic increasing (5) or flat (6) as the sources are located farther from the array. Unitary spikes, also captured in wide-band LFP recordings, may be segregated into independent components with activity in one/two recording sites (2). (B) The cytoarchitecture of the population defines the shape of the profile when recording close to it. While maxima typically occur at the synaptic band for inputs to laminar populations (e.g., the CA3 Schaffer input to the CA1, in blue), in curved populations the maxima may be at zones where there is a strong accumulation of passive currents even beyond the physical space of the generating neurons, such as in the hilus of the Dentate Gyrus (arrow) for excitatory inputs through the medial perforant pathway (mPP). Hatched bars mark the synaptic bands. (C) The spatial profiles of a given LFP generator may differ along the extension of the target population. Differences are however smooth and follow anatomical boundaries. (B, C) modified from Benito et al. (2014).

evaluating the values at all the electrodes at each instant following user-defined statistical criteria. The optimal solutions appear in the output matrix as reconstructed time series containing the relative amplitude of the spatial profile for each component or LFP-generator over time, which proves to be proportional to the varying intensity of the source.

Anatomical correlates of spatial profiles

Sampling three-dimensional voltage shells with linear probes. The spatial distribution of each LFP generator is unique and may serve to anatomically identify the generator, whereas the time course varies with the strength of the synaptic input and it can be used for quantitative studies (e.g., by correlating it with unit firing or behavior). Ideally, three-dimensional sampling of the voltage shell would best identify a LFP generator. While 3D linear arrays are under development, the most common linear arrays provide small samples of the voltage shell. Such linear spatial curves will differ for different placements (Fig. 6C). Thus, getting familiar with the spatial distribution of the LFP generators in relation to known anatomical landmarks is crucial, particularly as alterations in their expected shape may help identify errors in the application of the ICA or in defining the suitability of the data. Since the spatial and temporal parts of an ICA component are the two faces of the same coin, deviations detected in the spatial distribution necessarily imply alterations in the time course and vice versa (Makarova et al., 2011).

The profiles of six ICA-derived LFP generators have been considered depending on the position of the target neuronal sources (Fig. 6A). As a rule of thumb, linear or quasi-linear distributions (5 and 6) reflect remote sources that are generated in populations far from the recording sites, whereas bell-shaped distributions are typical of local (3) or nearby (1 and 4) sources. Flat distributions with a dip in one or at a few separated sites typically reflect spike activity, or a transient instability in one electrode, which can easily be recognized in the corresponding raw LFP channel. External artifacts appear as flat distributions (e.g., 50-Hz noise, switching artifacts, etc.).

The shape of the spatial distribution of an LFP generator reflects the sampling of the synaptic territory by an electrode array, although it is often not intuitive. For instance, synaptic inputs to planar populations yield LFP generators with simple spatial distributions that roughly mimic the synaptic territory of the afferent pathway and they normally only display one maximum there (Fig. 6B, blue trace). By contrast, glomerular populations are expected to produce smaller LFPs with non-intuitive spatial distributions and local maxima. In curved structures such as the dentate gyrus (DG) and cortical gyri the voltage profile may reflect architectonic features of the population rather than others related to

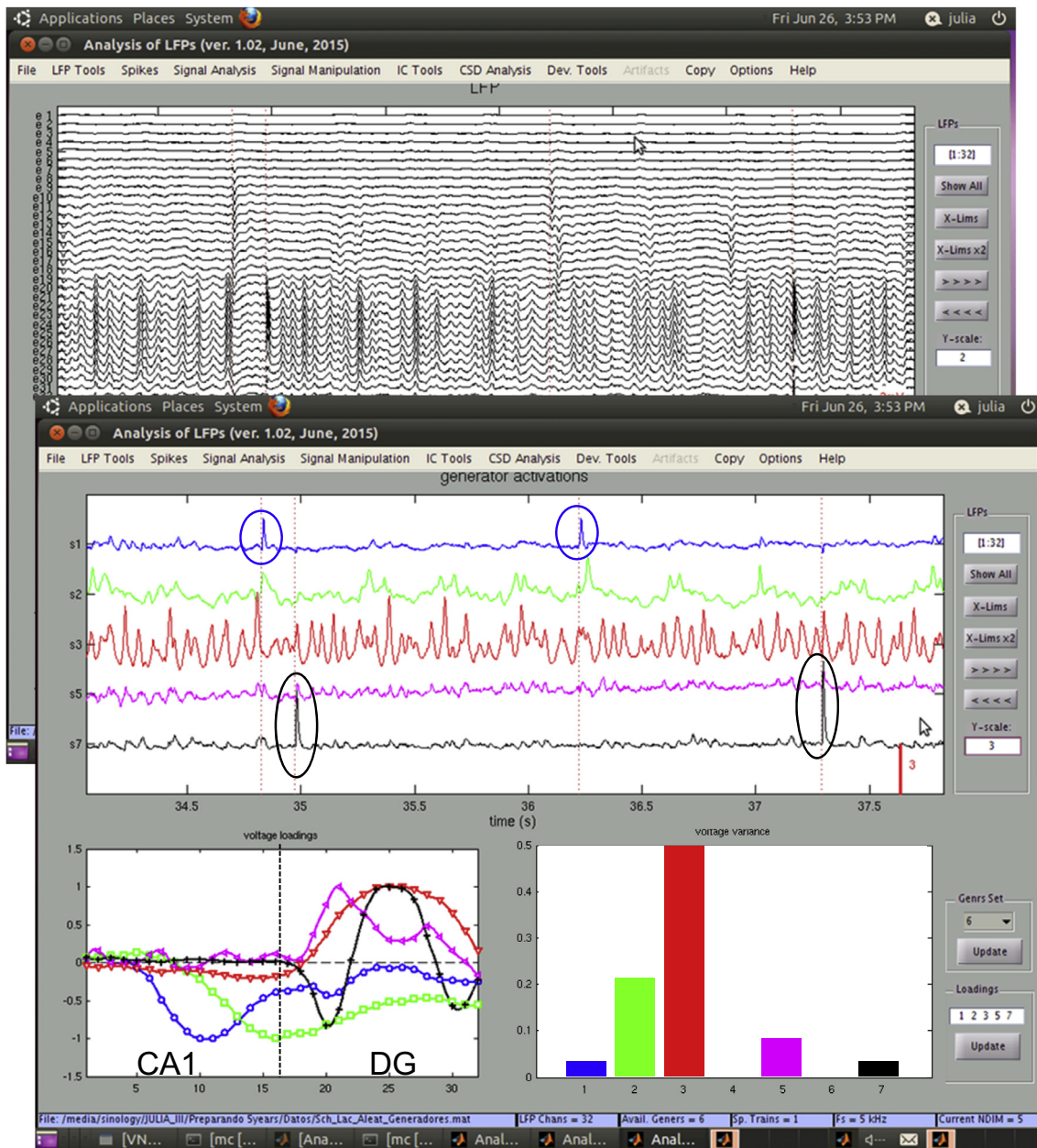


Fig. 7. Analysis of a sample epoch of LFPs recorded using a 32-channel linear array that spanned CA1 and CA3/DG subfields. The analysis was performed using Chen's (2006) kernel-density ICA algorithm implemented in the LFPsource® program running in MATLAB® environment. The upper half-screenshot shows the raw LFPs and the results are in the lower screenshot: the upper window presents the temporal activation of 5 main LFP generators whose spatial distribution is in the lower left window (electrode location goes left to right). The window on the right shows the relative variance of the LFP generators. Encircled spikelets correspond to evoked fEPSPs elicited by subthreshold stimuli applied to the ipsilateral CA3 (blue trace) and the medial perforant pathway (black trace), respectively, which appear in the corresponding LFP generator: evoked activity efficiently identifies the origin population of ICA-derived virtual LFP threads. Note the different time course of activities for the different LFP generators. Program available at <http://www.mat.ucm.es/~vmakarov/downloads.php>.

the cell morphology or the location of the synaptic input. The maximum may be displaced from the synaptic territory, even away from the post-synaptic cells generating the current, and the polarity may or may not reflect that of the synaptic current (e.g., Fig. 3D). For example, LFPs in the folded DG reach maximal amplitude at the interposed Hilus due to the clustering of passive currents from granule cells there, which oversize the clustering of active currents in the synaptic territory (Fig. 6B).

Several afferent pathways typically converge on the same target population, which may then produce many overlapping fields. Spatial overlapping also occurs when two different nearby populations (or even sharing a volume) receive distinct inputs. Despite the heavy spatial overlap, the ICA is capable of separating the inputs as it discriminates even small differences in the respective field potential gradients. Yet, optimal separation may require specific handling (Makarova et al., 2011; Schomburg et al., 2014; see below).

Obviously, two pathways that converge on the same sub-cellular location of the same population produce near-identical spatial profiles and will not be separated, a potential handicap for ICA usage. Such hybrid generators have been found for instance in the distal apical dendrites of hippocampal CA1 pyramidal cells (Benito et al., 2014).

Besides matching the spatial distribution of the LFP generators to anatomical data, additional functional tests may help identify the origin and target populations. Exogenous activation of axon bundles discriminates long-range excitatory projections well and then, evoked potentials appear in only one of the multiple LFP generators extracted from a single LFP profile (Fig. 7, encircled activity). In regular structures the chemical nature and synaptic territory can be disclosed by microinjection of excitatory and inhibitory neurotransmitter antagonists restricted to dendritic bands. Furthermore, the firing of units in suspected origin regions can be correlated with the temporal activation of LFP generators in a target region (spike-averages). Typically, afferent but not postsynaptic units exhibit significant correlations (Makarov et al., 2010; Fernández-Ruiz et al., 2012a; Martín-Vázquez et al., 2013).

Some weaknesses of ICA of LFPs: Intracellular blending of currents

The basis on which the ICA may separate the pathways contributing to LFPs is that each produces an extracellular electric field with a distinct and steady spatial distribution. Notably, the ICA algorithms are robust when discriminating overlapping fields produced by pathways terminating on different populations. However, the postsynaptic currents elicited by different pathways that converge on the same population interact *within* individual neurons and they modify each other's spread (Liu, 2004; Willadt et al., 2013), potentially compromising spatial stability. A variety of mechanisms may distort the expected spatial pattern of a given pathway, such as the internal cancelation of de- and hyperpolarizing currents, modification of their intracellular pathway through membrane shunts, or the addition of new currents by intrinsic V-dependent channels (Marder and Goaillard, 2006). A detailed model-assisted analysis has demonstrated that ICA algorithms converge on a unique spatial solution per component and dataset, reflecting the average of the synaptic inputs in multiple neurons plus whatever additional currents are recruited postsynaptically (Makarova et al., 2011). Importantly, ICA algorithms average out occasional and/or varied interactions between inputs, making this approach particularly suited for irregular activities, but possibly reducing the efficiency when interactions between inputs are very repetitive in the epoch analyzed. In extreme cases of two highly coherent activities in two inputs converging on a target population, an extra hybrid generator may appear in addition to the original pathway-specific ones. Such additional generators are difficult to identify as their spatial profile is defined by the morpho-electronic features of postsynaptic cells. Indeed, when hybrid generators achieve a significant vari-

ance they may even invalidate the time course of genuine ones.

Limitations of ICA for spatially shifting LFPs and hypersynchronous events

The ICA algorithms can be toggled for spatial, temporal or hybrid discrimination and it was shown that the use of combined spatio-temporal discrimination yields worse results (eşki et al., 2010). Indeed, only the spatial ICA fits the instantaneous character of electric fields in the brain (Makarov et al., 2010). By the same token, if the ICA is toggled for returning temporal or spatiotemporal motifs, pathway specificity cannot be warranted. However, spatial ICA is not practical in naturally occurring cases of spatially shifting LFP events. Some are originated by true propagating currents, such as unitary or population somatodendritic spikes (e.g., Herreras, 1990; Varona et al., 2000), while others belong to voltage shells elicited by combinations of nearby static current sources that activate with a slight temporal delay. In the case of lonely propagating events, the ICA returns several split components each with a unique but shifted spatial distribution, such as snapshots of a moving object taken by a high-speed camera (Korovaichuk et al., 2010). In the case of two nearby synaptic inputs, the efficiency of the ICA is determined by the proportion of co-varying time points (see Makarova et al., 2011; Martín-Vázquez et al., 2015).

Other modes of truly propagated current sources occur at the single-cell level and if they recur sufficiently, they may have a macroscopic manifestation. At least two intracellular mechanisms may underlie spatial shifts: the electrotonic conduction of synaptic currents across the cell (Rall, 1967) and the recruitment of slow intrinsic currents away from the synaptic zones (Herreras, 1990; Canals et al., 2005). In both cases the consequence is that the instantaneous V_o spatial profiles vary somewhat over the duration of the synaptic event. Electrotonic conduction produces a slight delay in the peak current, the membrane capacitance distancing it, as well as the return currents to the extracellular space, from the synaptic zones. The differences between the profiles of successive time instants are small and graded, and they are normally averaged into one. However, we have noticed that in particular cases of hypersynchronous activity, the instantaneous profiles may split into two or more groups with a similar but sufficiently discrepant distribution and the ICA separates them (Herreras and Makarova, unpublished observations). Such problems are uncommon in natural LFPs that present a high spatiotemporal jitter and weak synchronization, yet it may affect LFP epochs with a massive contribution of evoked potentials, or model LFPs synthesized from currents that are synchronous in all neurons (Korovaichuk et al., 2010; Makarova et al., 2011). Presumably, hypersynchronous synaptic events may split the spatial profiles in function of the different time constant in the initial moments, when the membrane resistance is shunted by ion currents, as compared to that in the later phases.

Hypersynchronous activity represents an additional challenge to the ICA approach, as it affects networks and populations that do not normally contribute

significantly to LFPs, yet where multiple and excessive co-activation becomes the rule. The different source composition may convey alterations in the global statistical properties, which given the excessive coherence between sources, may negatively affect the performance of the ICA. For instance, we have observed unstable results in the ripple fraction of hippocampal sharp waves and in epileptic phenomena.

APPLICATIONS OF PATHWAY-SPECIFIC LFP GENERATORS

Network dynamics: continuous parallel readouts of several population outputs

We shall now consider a series of objectives related to the exploration of network and population dynamics that LFP generators can address, some new and others re-appraised.

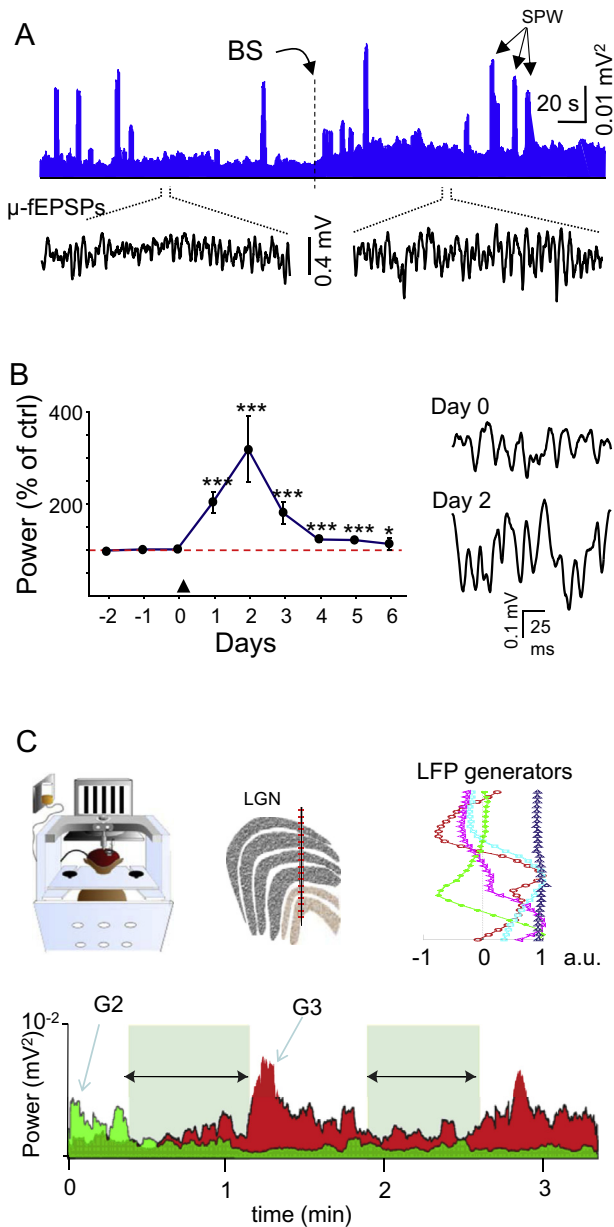
Access to information contained in irregular fluctuations. For decades, the literature on LFPs has focused on conspicuous and stereotypic activities and oscillatory patterns (Buzsáki et al., 1983; Vinogradova, 1985; Palva and Palva, 2007), while the information contained in irregular LFPs has been largely neglected. Nevertheless, irregular LFPs constitute the bulk of the activity in the brain (Jarosiewicz et al., 2002; Bullock et al., 2003), particularly if we consider that projection neurons in cortical structures fire sparsely and irregularly (Softky and Koch, 1993; Stevens and Zador, 1998). Therefore, irregular activity carries information that must also be explored, as it may reflect the temporal structure of natural incoming stimuli. While the regular or irregular pattern of the sources blended in an irregular LFP cannot be anticipated, irregular activity in a separated LFP generator can be safely interpreted as the postsynaptic convolution of irregular series of spike trains in one afferent population.

Grouping LFP events that originate in a common population. The firing of most neurons is essentially non-stationary and may reflect different regimes (such as cerebellar, hippocampal or cortical neurons: Fujisawa et al., 2006; Fernandez et al., 2007; Mazzucato et al., 2015). Different modes of firing will produce different synaptic envelopes in target cells (Ho et al., 2012), although spatial mixing with those elicited by other pathways may prevent the origin from being precisely determined. Indeed, a variety of spatiotemporal motifs can be appreciated in raw LFPs, and investigating their synaptic origin has been arduous and only occasionally successful. Despite intensive research, the cellular basis of some well-known LFP motifs remains controversial, such as that of the hippocampal theta rhythm, ripples, and the gamma oscillations in the cortex and hippocampus (Brankač et al., 1993; Fernández-Ruiz and Herreras, 2013; Schönberger et al., 2014). When several of these activities appear in a given LFP generator, their cellular basis can be safely unified and identified. For instance, the LFPs in the hippocampal CA1 region receive a contribution from the ipsilateral CA3–CA1 (Schaffer) LFP gen-

erator that displays two temporal patterns, bouts of 40-Hz gamma activity and sporadic sharp waves. These correspond to two different firing modes of the pyramidal CA3 population: the former to sequential firing of small functional assemblies that preserve a dominant lamellar topology; the latter produced by extended avalanche-like firing of CA3 pyramidal cells progressively moving over the longitudinal axis (Fernández-Ruiz et al., 2012a; Benito et al., 2014).

Assessing ongoing plasticity. Synaptic plasticity can be produced exogenously by repetitive electrical stimulation in a group of fibers, and the outcome can also be measured by evoked potentials using test stimuli (Bliss and Lomo, 1973). Although evoked activity serves to check the excitability of the postsynaptic population, it cannot evaluate changes in the ongoing activity through that pathway, either provoked by exogenous stimuli, experience-dependent, or associated with working memory mechanisms (Egorov et al., 2002; Whitlock et al., 2006; Takehara-Nishiuchi and McNaughton, 2008), and whether these changes are transmitted downstream (Martin and Shapiro, 2000). Estimations of the parameters in raw LFPs, such as power or frequency content, are inconclusive as they cannot be attributed to the pathway under study, or any other from local or distant projecting populations. Besides, the changes in the level of activity are not necessarily correlated with LFP power. However, such estimations can be easily achieved by following time envelopes of the LFP generators for which sustained changes of activity can be more easily converted into the output of the origin population. Moreover, the fine temporal details of pathway-specific individual waves may provide information as to the underlying network mechanisms. For instance, LTP protocols applied to the CA3 pyramidal population result in a sustained increase in Schaffer-specific activity entering the CA1 pyramidal population (Fig. 8A). This altered pathway flow is accompanied by a subtle reorganization of CA3 functional assemblies, and the enhanced influence of the Schaffer input on the firing of CA1 unitary spikes (Fernández-Ruiz et al., 2012b).

Long-term effects of pharmacological treatment, genetic differences and pathology. A promising use of LFP generators is to investigate the alterations produced during drug treatment or pathology. For instance, we have been able to examine the activity in the Schaffer CA3–CA1 pathway over several days in animals treated chronically with drugs that promote the growth of dendritic spines, assessing network functionality on successive days while the animal performs behavioral tasks (Enríquez-Barreto et al., 2013; Fig. 8B). In addition, the expansion of abnormal activity in the network initiated in a structure/population can be followed downstream by examining the sustained activity of LFP generators at successive stations. Further applications include the testing of the effects of genetic manipulations used to establish animal models of cognitive deficit. In such circumstances, LFP generators may provide sustained alterations in the mean activity of



certain pathways, whether central or subsidiary to the experimental manipulation.

Exploring population activities over different time scales. The stability of experimental variables over extended periods may represent a handicap in long-term studies. Indeed, the activity of a neural population undergoes rapid changes due to the instantaneous processing demands during task execution, or the sustained long-term modulation related to the animal's state, or to circadian and other hormone-derived cycles, during development or throughout life (Salami et al., 2012; An et al., 2014). To date, studies into the cellular basis of behavior have relied mostly on multiunit analyses and they focus on task-related time references that are imprecise in terms of neuron firing. In addition, a single unit may belong to several functional assemblies and its spike activity is poorly representative of natural

transmission that is largely based on functional assemblies (Eckhorn and Obermueller, 1993; Sakurai et al., 2013), and whose synchronous firing produces LFPs downstream. LFP generators provide a unique means to check for alterations to ongoing activity in several identified populations over different time scales. In the short term, the changes in individual waves (e.g., amplitude and duration) reflect the size and synchronization of cell assemblies in the afferent population (Fernández-Ruiz et al., 2012a), while frequency alterations also reflect changes in local networks in the afferent region, such as CA3 GABAergic interneurons setting the pace in CA3–CA1 gamma bouts (Lasztóczy and Klausberger, 2014). Over longer time scales (minutes to hours), LFPs exhibit changes in their mean activity according to the animal's state, such as still vs. alert, quiet vs. resting, in motion or asleep (see Makarova et al., 2014 and Fig. 8C).

Active networks in different brain states. An emergent concept in the contemporary literature is that of global brain states that are viewed as default modes for the operation of certain brain networks (Gervasoni et al., 2004) and that underlie state-dependent information processing (Leung, 1980; Herreras et al., 1988; Edeline et al., 2000). These states have been classified using gross parameters of brain activity, such as the correlation of spectral features of LFPs in several brain regions. A common problem is that the participating pathways and networks cannot be safely derived from raw LFPs that may have a strong contribution from volume-conducted fields. This problem is absent with pathway-specific generators where the location of the source is known by the shape of the spatial distributions. Thus, functional connectivity is more safely assessed by comparing the mean

Fig. 8. Some applications of LFP generators to the study of network activity. (A) Sustained alterations of ongoing activity following long-term potentiation inducing protocols. The plot shows a temporal envelope of the Schaffer generator before and after theta burst stimulation (BS). Note the increase in mean activity through the Schaffer pathway under unstimulated conditions. The samples below show the dominant gamma activity, termed micro-fEPSPs in this generator. Individual waves augmented in amplitude, but their duration and frequency remained stable after LTP. Sharp waves (SPW) also appeared in this generator as they are produced in the CA1 by CA3 firing. (B) Long-term study in chronically implanted animals. The plot shows the power of the Schaffer generator extracted from linear profiles of LFPs across the CA1 layers before and after hippocampal injection (at day 0) of a PI3K activator that promotes the formation of new spines. Note the transient increase 1–3 days after drug injection. Individual gamma waves or micro-fEPSPs increased in amplitude but not in frequency or duration. (C) Evaluation of the activity in multiple populations over long periods and in different behavioral states. LFP generators (upper right colored plots) were obtained from linear LFP recordings in the lateral geniculate nucleus (LGN) of a monkey while performing a visual task. The blue trace belongs to a remote source as it entered a similar power to all electrodes. All others have maxima in different layers, indicating different afferent pathways with local synaptic territories. The evolution of the power in the two LFP generators (lower panel) shows specific alterations related to the behavioral states. The periods marked by horizontal arrows coincide with eye closure and somnolence. (A) From Fernández-Ruiz et al. (2012a); (B) from Enríquez-Barreto et al. (2013); (C) modified from Makarova et al. (2014).

levels and fine temporal details of the waves in pathway-specific generators of different structures than by correlating single-point raw LFPs in different structures that may receive the contribution of unknown mixtures of unknown populations.

Cellular and biophysical mechanisms

A number of issues related to the cellular basis of LFPs can now be addressed by LFP generators that are not accessible from raw LFPs. Two such classical problems already mentioned are the unknown origin of the afferent populations and the extreme variation in the activation of the contributing pathways. Using LFP generators, our group has obtained direct empirical support for a number of theoretical concepts developed long ago but that were difficult to assess experimentally. The LFP generators grant homogeneity in the population of origin, and the corresponding spatial shells of V_o can be matched to anatomical landmarks, in some cases with subcellular accuracy. Also, the shifting nature of LFPs is no longer a problem but rather, the uncontaminated temporal fluctuations of LFP-generators can be interpreted as a convolution of afferent spike trains from a homogeneous population, and interpreted as a function of the size, synchrony and temporal pattern of firing by functional neuron assemblies. A few examples illustrating these advantages are listed below, some of which reiterate issues already introduced above but delving deeper into the more mechanistic and technical aspects.

Identifying the true polarity and amplitude of pathway-specific postsynaptic currents. One important problem when identifying the nature of an LFP oscillation is that removing the DC components from standard (AC-coupled) recordings also gets rid of the baseline, eliminating the possibility of inferring the polarity of the currents underlying sine-wave oscillations (Brankačk et al., 1993). It also affects irregular LFPs, since AC-coupling acts separately on LFPs recorded by each electrode and distorts their spatial relation. As a consequence, the standard current source density (CSD) approach (Lorente de Nó, 1947; Freeman and Nicholson, 1975) renders spurious succession of sources and sinks for oscillatory LFPs (Bragin et al., 1995; Castro-Alamancos, 2000) and it produces a noisy background of spurious currents for irregular ones (Fernández-Ruiz et al., 2012a,b). Moreover, as co-activated currents elicited by different inputs onto adjacent sites play an effect of mutual envelope, they hamper the identification of excitatory or inhibitory currents in spatial maps. These problems have no solution for multi-origin LFPs but they can be strongly reduced for pathway-specific ones that generate a unique spatial voltage distribution, as is the case for some evoked potentials. One solution has been proposed that first isolates the pathway-specific input conveying the oscillatory (or irregular) fields through the use of the ICA and then, the correct polarity is recovered through site-specific baseline rectification (Martín-Vázquez et al., 2013).

LFP polarity does not identify excitation or inhibition. There is a widespread belief that negative and positive LFPs reflect excitatory and inhibitory currents, respectively. This misconception comes from ill-posed unit-to-population analogies, often evident in the crude interpretations of the peaks and valleys of LFP oscillations mentioned above. Frequently these are interpreted as representing excitatory–inhibitory sequences in analogy to the intracellular EPSP–IPSP sequences found in intracellular recordings following exogenous activation. Although it is possible to access the relative contribution of background excitatory or inhibitory currents to the somatic membrane potential fluctuations in single cells (Rudolph et al., 2007; Greenhill et al., 2014) one cannot expect this relationship to be maintained in LFPs that are dominated by dendritic currents that may or may not produce extracellular fields. Besides, synaptic inputs whether excitatory or inhibitory, produce LFPs of both polarities but in different loci (Fig. 3C), which can be boosted unevenly by cytoarchitectonic and other factors. Computer-assisted forward solutions of synthetic LFPs for pathway-specific inputs reveal that the dominant polarity of LFPs actually depends on the site of input over the somatodendritic axis and the population architecture, rather than on the chemical nature of the input. Indeed, excitatory and inhibitory inputs may both lead to dominant positive LFPs in curved structures if they impinge on different parts of the neuron (Fig. 3D). These effects are brought about by volume conduction in concert with population architecture. Yet volume conduction not only plays a decisive role in folded laminae but it is also instrumental in planar structures, which is particularly evident when two regions receive coherent inputs. The dipolar fields generated in one region may be severely distorted by concurrent distant dipoles oriented differently, which may alter hallmarks of LFPs, such as the dominant polarity, site of polarity reversal, and the amplitude (Martín-Vázquez et al., 2015).

Discriminating local and volume-conducted contributions. Some of the computational results that highlight the multiple roles of volume conduction have already received experimental support and they jointly represent a promising step toward the objective of scaling LFPs that are produced by many deep local sources, to the EEG. Separate treatment of deep sources appears to also be more advantageous for this purpose. As previously noted, raw LFPs rarely identify what comes from where, which may provoke incorrect interpretations of the correlations observed between signals recorded in different regions. Some numerical techniques, like CSD analysis, may in principle discriminate local contributions as they eliminate volume-conducted currents (Freeman and Nicholson, 1975). While this has been validated for numerous evoked field potential profiles (Mitzdorf and Singer, 1977; Rodríguez and Haberly, 1989; Herreras, 1990), CSD is unsuitable for standard AC-coupled LFP recordings in which a large fraction of the estimated current is spurious (see above and Martín-Vázquez et al., 2013). This problem does not affect the spatial distribution of an LFP generator obtained through the ICA as the tem-

poral content is identical whether recorded locally or at remote sites.

Identifying pre- and postsynaptic units in spike-phase plots. Spike-phase plots are often used to explore the relationship of units to the concomitant LFP waves (e.g., [Murthy and Fetz, 1996](#)). Since the baseline of waves in raw LFPs is unknown, the plots use phase angles that do not allow causal relationships to be established between the firing unit and the LFP studied. In these, the spike time is used as a reference to average LFP waves. Instead, by using the time course of a pathway-specific generator, the starting time and polarity of individual pathway-specific waves (a selected fraction of the total) can be unequivocally established and used as zero-time reference. The resultant spike-wave plots shift the activity over the wave and they become net left or right sided for afferent or postsynaptic units, respectively ([Martín-Vázquez et al., 2013](#)). Importantly, the duration and form of individual waves in pathway-specific LFPs is comparable to that of elementary synaptic currents in postsynaptic cells in many cases, such as the ongoing micro-field excitatory postsynaptic potentials (f-EPSPs) making gamma waves in the CA1 stratum radiatum driven from CA3 pyramidal cells ([Fernández-Ruiz et al., 2012a](#)). The time-course of waves can thus be used directly so avoiding the complications of phase measurement and interpretation ([Lopes da Silva, 2006](#)).

Identifying the topology of connections through spatial modules of coherent activity. The fibers connecting two structures are often arranged in a topological manner so that sections of an afferent population contact different regions of the postsynaptic target. Since the activity flows through varying groups of axons, the resultant LFPs will differ in separate loci of the target population, yet they are still captured by the same pathway-specific LFP generator. By examining the coherence between readouts of the same generator at different sites, one may delimit the extent of the targeted tissue that is co-activated by synchronous afferent activity. Some such spatial modules of coherent LFPs arise from the overlap of axonal territories setting common spatial boundaries for synaptic currents elicited by homogeneous afferent neurons, while others appear to arise from the spatial merging of independent axonal territories of synchronously activated inhibitory neurons ([Benito et al., 2014](#)).

TECHNICAL ASPECTS OF ICA USAGE ON LFPs: HINTS AND WORKAROUNDS

Some general considerations

The performance of ICA on LFPs is evaluated in terms of how well it separates mixed sources, even though they are unknown *a priori*. The results should be considered statistical solutions to a problem ([Bell and Sejnowski, 1995](#); [Stone et al., 2002](#); [Choi et al., 2005](#)) and although unexpected observations may be judged as defects in the tool, they may actually be due to inadequate signal handling. Learning to evaluate how the ICA solutions

match available anatomical and functional data and whether they fulfill theoretical knowledge and expectations goes in parallel to the understanding of LFP biophysics.

The temporal accuracy of an LFP generator is proportional to its relative presence in the sample ([Makarova et al., 2011](#)). The solutions rendered by the ICA are statistical estimates *that necessarily depend on the sample* and therefore, when the LFP epoch contains long segments with obvious differences in the composition of the contributing sources, some changes to the dataset such as the length of the epoch or the group of sites used to build the LFP matrices, might alter the set of sources found or their accuracy. In practice, it is convenient to repeat the analysis with different algorithms and/or preprocessing of the dataset. In our experience, benchmarking the ICA on synthetic LFPs is particularly beneficial to establish useful ranges and limits.

Preprocessing: goods and bads

The removal of ultraslow (DC-coupled) potentials. Slow field potentials (< 1 Hz) may have a real or artifactual origin, and they should be removed with caution as they may be useful in some cases or impose further difficulties in others. Slow potentials contribute the largest amount of variance to LFP signals and hence, they facilitate the convergence of ICA algorithms and they increase the accuracy of the fluctuations in the underlying pathways. Even if artifacts are well separated by the ICA into other components ([Castellanos and Makarov, 2006](#)), they contribute a large amount of variance and reduce the contribution of signals, which may lead to cross-contamination particularly of the weaker generators.

Filtering. A most frequent pretreatment of LFPs is band-pass filtering, either to reduce noise or to emphasize desired aspects of the time course. While filtering is a powerful tool, it has a number of frequently neglected drawbacks when exploring bioelectrical signals and thus, it should be used with caution. The main drawbacks of filtering LFPs prior to ICA are: (1) band-pass filtering eliminates the main advantage of ICA on LFPs, namely, the access to information regarding population dynamics contained in *irregular* LFP activity, which reflects the stochastic nature of natural stimuli (it should be noted that most if not all populations that fire on rhythmic regimes may also fire irregularly: [Bullock et al., 2003](#)); (2) filtering alters the time course of LFP generators that contain interspersed epochs of rhythmic and irregular activity inconsistently; (3) high-pass filtering weakens LFP generators by removing their low-frequency components, whose stronger energy (variance) facilitates the convergence of the algorithms. Thus, filter-weakened generators become more susceptible to cross-contamination; (4) importantly, filtering often distorts the spatial curve of the ICA components obtained, making the afferent pathway unrecognizable ([Korovaichuk, 2012](#)). In principle, post-ICA filtering of

the generator's time course is less dangerous as it already contains activity from a single pathway.

The reduction in dimensionality. Ideally, each LFP generator is contributed by only one synaptic pathway and thus, only a few components will explain most of the variance (~99%) whereas the remaining components are “noisy-like” (Makarov et al., 2010). However, it is not uncommon that LFP generators split into two or more ICA components, while hybrid components appear less frequently (i.e.: two pathways are blended into a single component). Some causes of this are mentioned below but to a great extent, they can be prevented by reducing the dimensions prior to performing the ICA by using a principal component analysis (PCA). This has become a customary step and it has been shown not to distort the original signals.

Hints: maximizing the contribution of the source of interest

The LFP generators derived by applying ICA to a dataset may have distinct accuracies, a factor that is most strongly influenced by the quantitative contribution of each source to the mixture (i.e., their relative variance). Nearly all the hints described below seek to optimize the weaker generators. As already stated, recognizing the spatial curves and their variants is essential, and indeed, blurry, jumpy and generally unsmooth spatial curves are a sign of insufficient separation.

Repeated analyses of the same LFP epochs using different groups of channels. An efficient way to check for the reliability of a set of generators is to compare the fine temporal details in different runs of the ICA over the same LFP epoch after discretionarily removing some of the original channels. The different data sets make the algorithm work on different LFP matrices that contain the same temporal dynamics, albeit with different weights. Therefore, matching the temporal details in different trials has a strong confirmatory value of the efficient separation of a given generator.

Optimizing the electrode placement. The number of electrodes may be relevant to improve separation (Glabska et al., 2014) but in all cases, it is central to span relevant sites. Given the high sensitivity of the ICA, the optimal choice of recording sites does not necessarily include those where the source of interest has stronger amplitude but rather, those where it overlaps less with other sources while still retaining significant variance (Fig. S3 in Benito et al., 2014). In orderly populations it is important to record from the most planar and homogeneous sections, and avoid recording from edges and sites of strong curvature. If these cannot be spared, a way to improve the separation from nearby generators is to record simultaneously from several linear tracks. The multiple spatial references thereby included in the loading matrix for each generator facilitate convergence and reduce cross-contamination.

Linear recording arrays may span several structures or subfields, encompassing several neuron populations,

and each of them may be the target for LFP contributing inputs and also the origin of other generators themselves. In some structures the cell generators may be physically segregated (e.g., the pyramidal and granule cells in CA1/DG hippocampal subfields), and in others multiple cell types may occupy the same region (e.g., cortex, lateral geniculate nucleus; Fig. 1). One may choose to build an LFP matrix using the recording sites spanning only one population while leaving out contiguous sites. While this procedure may increase the relative contribution of local sources, it should be performed with caution as the nearby sources omitted still enter volume-conducted activity to the recorded region that is then directed to weakened generators. Hence, when working on a spatially reduced matrix, the ICA has less chance of efficiently discriminating generators and their activity may be incorporated into a local source, which becomes contaminated. While weak nearby sources with irregular activity are efficiently separated, it may be troublesome when the temporal courses of local and nearby generators both have an oscillatory content with a similar frequency, such as during gamma oscillations in the DG and distal CA1 layer (Schomburg et al., 2014). In such cases separation can be optimized by the joint analysis of the two regions so as to reinforce the variance in all generators (Benito et al., 2014).

Priming the pathway of interest. Weak LFP generators are so because either cytoarchitectonic features are not optimal for charge separation in the extracellular space, or because the afferent population has an inadequate temporal regime (e.g., sparse or too intense and regular activations, Ho et al., 2012). An efficient way of increasing the variance of a weak generator is to add exogenous evoked activity through electrical pulses to the afferent pathway (Korovaichuk et al., 2010). This has several benefits, such as increasing the total contribution of a pathway to a given LFP epoch, making its separation more reliable. In addition, it is a safe test for pathway specificity as the evoked potential should appear in only one ICA component (Fig. 6).

CONCLUDING REMARKS: A NEW ERA FOR LFPS

The pioneers in the study of LFPS pointed out that the spatial complexity of the source elements is the main handicap to understand the cellular basis of “brain waves”. Although the lack of precise microscopic details of individual neurons is less relevant at the macroscopic level in which LFPS develop, some such features are essential to determine the amplitude, polarity and reach, and they define characteristic spatial profiles. Spatial discrimination techniques can capture these and separate them, providing a full temporal account of their independent activities. The application to real LFPS is not free of complications and the sources of cross-contamination have to be carefully observed. However, in the worst of cases the specificity is far greater than in raw LFPS. Future work should address technical issues

aiming to improve the reliability of weak LFP generators, such as designing new algorithms that are specific to the statistical properties of LFPs, establishing adequate protocols to estimate cross-contamination, or defining spatial templates that can be used as primers for ICA algorithms.

All in all, the availability of pathway-specific LFP generators shall prove advantageous in applied Neuroscience, e.g. as possible signals to be used in brain–machine interfaces (Andersen et al., 2004). They shall also foster the experimental exploration of long-standing questions, such as why some pathways but not others produce LFPs, more simple problems like understanding why an LFP is positive or negative, or those more puzzling ones, such as how an LFP can be larger when it is further away from its source. If we cannot obtain responses to these questions, we will be unable to adequately address many other questions that bridge the gap between unitary and macroscopic electrogenesis. In TH Bullock's words "there is a lot of micro- as well as macrostructure in the activity" (1997). Obtaining continuous readouts of the activities of several populations opens new avenues that will not just help binding the different functional levels of electrical activity but also how these yoke together with changing micro- and macrostructure through lifespan and define network dynamics in animals performing specific behaviors or carrying pathological alterations associated with known biophysical and cellular changes.

Acknowledgements—We thank A. Korovaichuk, N. Benito and G. Martín-Vázquez for continual discussion. We also thank S. Canals, M. Morales, T. Ortuño, D. Torres, and L. Pérez for useful comments on a previous version of the manuscript, and M. Sef-ton at BiomedRed for editorial support. This work was supported by Grants BFU2013-41533R to O.H. and FIS2014-57090-P to V.A.M. from the Spanish Ministry of Economy and Competitiveness.

REFERENCES

- An S, Kilb W, Luhmann HJ (2014) Sensory-evoked and spontaneous gamma and spindle bursts in neonatal rat motor cortex. *J Neurosci* 34:10870–10883.
- Andersen RA, Musallam S, Pesaran B (2004) Selecting the signals for a brain-machine interface. *Curr Opin Neurobiol* 14:720–726.
- Bedard C, Kroger H, Destexhe A (2004) Modeling extracellular field potentials and the frequency-filtering properties of extracellular space. *Biophys J* 86:1829–1842.
- Belitski A, Gretton A, Magri C, Murayama Y, Montemurro MA, Logothetis NK, Panzeri S (2008) Low-frequency local field potentials and spikes in primary visual cortex convey independent visual information. *J Neurosci* 28:5696–5709.
- Bell A, Sejnowski T (1995) An information-maximization approach to blind separation and blind deconvolution. *Neural Comput* 7:1129–1159.
- Beltramo R, D'Urso G, Dal Maschio M, Farisello P, Bovetti S, Clovis Y, Lassi G, Tucci V, De Pietri Tonelli D, Fellin T (2013) Layer-specific excitatory circuits differentially control recurrent network dynamics in the neocortex. *Nat Neurosci* 16:227–234.
- Benito N, Fernández-Ruiz A, Makarov VA, Makarova J, Korovaichuk A, Herreras O (2014) Spatial blocks of coherent pathway-specific LFPs in the hippocampus reflect different modes of presynaptic synchronization. *Cereb Cortex* 24:1738–1752.
- Bliss T-V, Lømo T (1973) Long-lasting potentiation of synaptic transmission in the dentate area of the anaesthetized rabbit following stimulation of the perforant path. *J Physiol* 232:331–356.
- Bragin A, Jandó G, Nádasdy Z, Hetke J, Wise K, Buzsáki G (1995) Gamma (40–100 Hz) oscillation in the hippocampus of the behaving rat. *J Neurosci* 15:47–60.
- Brankač J, Stewart M, Fox SE (1993) Current source density analysis of the hippocampal theta rhythm: associated sustained potentials and candidate synaptic generators. *Brain Res* 615:310–327.
- Bullock TH (1997) Signals and signs in the nervous system: the dynamic anatomy of electrical activity is probably information-rich. *Proc Natl Acad Sci* 94:1–6.
- Bullock TH, Mcclune MC, Enright JT (2003) Are the electroencephalograms mainly rhythmic? Assessment of periodicity in wide-band time series. *Neuroscience* 121:233–252.
- Buzsáki G, Leung LW, Vanderwolf CH (1983) Cellular bases of hippocampal EEG in the behaving rat. *Brain Res* 287:139–171.
- Buzsáki G, Anastassiou C, Koch C (2012) The origin of extracellular fields and currents—EEG, ECoG, LFP and spikes. *Nat Rev Neurosci* 13:407–420.
- Canals S, López-Aguado L, Herreras O (2005) Synaptically-recruited apical currents are required to initiate axonal and apical spikes in hippocampal pyramidal cells: modulation by inhibition. *J Neurophysiol* 93:909–918.
- Castellanos NP, Makarov VA (2006) Recovering EEG brain signals: artifact suppression with wavelet enhanced independent component analysis. *J Neurosci Methods* 158:300–312.
- Castro-Alamancos MA (2000) Origin of synchronized oscillations induced by neocortical disinhibition in vivo. *J Neurosci* 20:9195–9206.
- Chen A (2006) Fast kernel density independent component analysis. *Lecture Notes Comput Sci* 3889:24–31.
- Choi S, Cichocki A, Park HM, Lee SY (2005) Blind source separation and independent component analysis: A review. *Neur Inf Process Let Rev* 6:1–57.
- Chrobak JJ, Buzsáki G (1998) Gamma oscillations in the entorhinal cortex of the freely behaving rat. *J Neurosci* 18:388–398.
- Comon P (1994) Independent component analysis, a new concept? *Signal Processing* 36:287–314.
- Cooper R, Winter AL, Crow HJ, Walter WG (1965) Comparison of subcortical, cortical and scalp activity using chronically indwelling electrodes in man. *Electroencephalogr Clin Neurophysiol* 18:217–228.
- de Cheveigné A, Edeline JM, Gaucher Q, Gourévitch B (2013) Component analysis reveals sharp tuning of the local field potential in the guinea pig auditory cortex. *J Neurophysiol* 109:261–272.
- DeLucchi MR, Garoutte B, Aird RB (1962) The scalp as an electroencephalographic average. *Electroenceph Clin Neurophysiol* 14:191–196.
- Dement W, Kleitman N (1957) Cyclic variations in EEG during sleep and their relation to eye movements, body motility and dreaming. *Electroenceph Clin Neurophysiol* 9:673–690.
- Destexhe A, Contreras D, Steriade M (1999) Spatiotemporal analysis of local field potentials and unit discharges in cat cerebral cortex during natural wake and sleep states. *J Neurosci* 19:4595–4608.
- Eckhorn R (1994) Oscillatory and non-oscillatory synchronizations in the visual cortex and their possible roles in associations of visual features. *Prog Brain Res* 102:405–426.
- Eckhorn R, Obermueller A (1993) Single neurons are differently involved in stimulus-specific oscillations in cat visual cortex. *Exp Brain Res* 95:177–182.
- Edeline JM, Manunta Y, Hennevin E (2000) Auditory thalamus neurons during sleep: changes in frequency selectivity, threshold, and receptive field size. *J Neurophysiol* 84:934–952.
- Egorov AV, Hamam BN, Fransén E, Hasselmo ME, Alonso AA (2002) Graded persistent activity in entorhinal cortex neurons. *Nature* 420:173–178.
- Elul R (1971) The genesis of the EEG. *Int Rev Neurobiol* 15:228–272.

- Enríquez-Barreto L, Cuesto G, Domínguez-Iturza N, Gavilán E, Ruano D, Sandi C, Fernández-Ruiz A, Martín-Vázquez G, Herreras O, Morales M (2013) Learning improvement after PI3K activation correlates with de novo formation of functional small spines. *Front Mol Neurosci* 6:54.
- Fernandez FR, Engbers JD, Turner RW (2007) Firing Dynamics of Cerebellar Purkinje Cells. *J Neurophysiol* 98:278–294.
- Fernández-Ruiz A, Herreras O (2013) Identifying the synaptic origin of ongoing neuronal oscillations through spatial discrimination of electric fields. *Front Comput Neurosci* 7:5.
- Fernández-Ruiz A, Makarov VA, Benito N, Herreras O (2012a) Schaffer-specific local field potentials reflect discrete excitatory events at gamma frequency that may fire postsynaptic hippocampal CA1 units. *J Neurosci* 32:5165–5176.
- Fernández-Ruiz A, Makarov VA, Herreras O (2012b) Sustained increase of spontaneous input and spike transfer in the CA3-CA1 pathway following long term potentiation in vivo. *Front Neural Circuits* 6:71.
- Fernández-Ruiz A, Muñoz S, Sancho M, Makarova J, Makarov VA, Herreras O (2013) Cytoarchitectonic and dynamic origins of giant positive LFPs in the Dentate Gyrus. *J Neurosci* 33:15518–15532.
- Freeman JA, Nicholson C (1975) Experimental optimization of current source-density technique for anuran cerebellum. *J Neurophysiol* 38:369–382.
- Fuentealba P, Timofeev I, Bazhenov M, Sejnowski TJ, Steriade M (2005) Membrane bistability in thalamic reticular neurons during spindle oscillations. *J Neurophysiol* 93:294–304.
- Fujisawa S, Matsuki N, Ikegaya Y (2006) Single neurons can induce phase transitions of cortical recurrent networks with multiple internal states. *Cereb Cortex* 16:639–654.
- Gervasoni D, Lin SC, Ribeiro S, Soares ES, Pantoja J, Nicolelis MA (2004) Global forebrain dynamics predict rat behavioral states and their transitions. *J Neurosci* 24:11137–11147.
- Gąbska H, Potworowski J, eški S, Wójcik DK (2014) Independent components of neural activity carry information on individual populations. *PLoS One* 9(8):e105071.
- Gloor P (1985) Neuronal generators and the problem of localization in electroencephalography: the application of volume conductor theory to electroencephalography. *J Clin Neurophysiol* 2:327–353.
- Goldwyn JH, Mc Laughlin M, Verschooten E, Joris PX, Rinzel J (2014) A model of the medial superior olive explains spatiotemporal features of local field potentials. *J Neurosci* 34:11705–11722.
- Gratiy SL, Devor A, Einevoll GT, Dale AM (2011) On the estimation of population-specific synaptic currents from laminar multielectrode recordings. *Front Neuroinform* 5:32.
- Gray CM, König P, Engel AK, Singer W (1989) Oscillatory responses in cat visual cortex exhibit inter-columnar synchronization which reflects global stimulus properties. *Nature* 338:334–337.
- Greenhill SD, Chamberlain SE, Lench A, Massey PV, Yuill KH, Woodhall GL, Jones RS (2014) Background synaptic activity in rat entorhinal cortex shows a progressively greater dominance of inhibition over excitation from deep to superficial layers. *PLoS ONE* 9(1):e85125.
- Haider B, Häusser M, Carandini M (2013) Inhibition dominates sensory responses in the awake cortex. *Nature* 493:97–100.
- Herreras O (1990) Propagating dendritic action potential mediates synaptic transmission in CA1 pyramidal cells in situ. *J Neurophysiol* 64:1429–1441.
- Herreras O, Solís JM, Muñoz MD, Martín del Río R, Lerma J (1988) Sensory modulation of hippocampal transmission. I. Opposite effects on CA1 and dentate gyrus synapses. *Brain Res* 461:290–302.
- Ho EC, Strüber M, Bartos M, Zhang L, Skinner FK (2012) Inhibitory networks of fast-spiking interneurons generate slow population activities due to excitatory fluctuations and network multistability. *J Neurosci* 32:9931–9946.
- Hyvärinen A, Karhunen J, Oja E (2001) Independent Component Analysis. John Wiley & Sons.
- Jacobs J, Kahana MJ (2010) Direct brain recordings fuel advances in cognitive electrophysiology. *Trends Cogn Sci* 14:162–171.
- Jarosiewicz B, McNaughton BL, Skaggs WE (2002) Hippocampal population activity during the small-amplitude irregular activity state in the rat. *J Neurosci* 22:1373–1384.
- Korovaichuk A (2012), Disentanglement of LFP contributions according to the afferent populations and its application to the study of networks dynamics in the hippocampus. Doctoral dissertation, University Complutense of Madrid.
- Korovaichuk A, Makarova J, Makarov VA, Benito N, Herreras O (2010) Minor contribution of principal excitatory pathways to hippocampal LFPs in the anesthetized rat: a combined independent component and current source density study. *J Neurophysiol* 104:484–497.
- Kreiman G, Hung CP, Kraskov A, Quiroga RQ, Poggio T, DiCarlo JJ (2006) Object selectivity of local field potentials and spikes in the macaque inferior temporal cortex. *Neuron* 49:433–445.
- Lasztóci B, Klausberger T (2014) Layer-specific GABAergic control of distinct gamma oscillations in the CA1 hippocampus. *Neuron* 81:1126–1139.
- eški S, Kublik E, Swiejkowski DA, Wrobel A, Wojcik DK (2010) Extracting functional components of neural dynamics with independent component analysis and inverse current source density. *J Comput Neurosci* 29:459–473.
- eški S, Lindén H, Tetzlaff T, Pettersen KH, Einevoll GT (2013) Frequency dependence of signal power and spatial reach of the local field potential. *PLoS Comput Biol* 9(7):e1003137.
- Leung LS (1980) Behavior-dependent evoked potentials in the hippocampal CA1 region of the rat. I. Correlation with behavior and EEG. *Brain Res* 198:95–117.
- Lindén H, Tetzlaff T, Potjans TC, Pettersen KH, Grün S, Diesmann M, Einevoll GT (2011) Modeling the spatial reach of the LFP. *Neuron* 72:859–872.
- Liu G (2004) Local structural balance of functional interaction of excitatory and inhibitory synapses in hippocampal dendrites. *Nat Neurosci* 7:373–379.
- Liu J, Newsome WT (2006) Local field potential in cortical area MT: stimulus tuning and behavioral correlations. *J Neurosci* 26:7779–7790.
- Lopes da Silva F (2006) Event-related neural activities. What about phase? *Prog Brain Res* 19:3–17.
- Lopes da Silva F, Van Rotterdam A (1982) Biophysical aspects of EEG and EMG generation. In: Niedermeyer E, Lopes da Silva F, editors. *Electroencephalography: basic principles, clinical applications and related fields*. Baltimore: Lippincott, Williams and Wilkins. p. 15–26.
- López-Aguado L, Ibarz JM, Varona P, Herreras O (2002) Structural inhomogeneities differentially modulate action currents and population spikes initiated in the axon or dendrites. *J Neurophysiol* 88:2809–2820.
- Lorente de Nó R (1947) Analysis of the distribution of action currents of nerves in volume conductors. In: *A Study of Nerve Physiology*, vol. 132. New York: The Rockefeller Institute. p. 384–477. Part 2.
- Makarov VA, Makarova J, Herreras O (2010) Disentanglement of local field potential sources by independent component analysis. *J Comp Neurosci* 29:445–457.
- Makarova J, Ibarz JM, Makarov VA, Benito N, Herreras O (2011) Parallel Readout of Pathway-Specific Inputs to Laminated Brain Structures. *Front Syst Neurosci* 5:77.
- Makarova J, Ortuño T, Korovaichuk A, Cudeiro J, Makarov VA, Rivadulla C, Herreras O (2014) Can pathway-specific LFPs be obtained in cytoarchitecturally complex structures? *Front Syst Neurosci* 8:66.
- Marder E, Goaillard JM (2006) Variability, compensation and homeostasis in neuron and network function. *Nat Rev Neurosci* 7:563–574.
- Martin PD, Shapiro ML (2000) Disparate effects of long-term potentiation on evoked potentials and single CA1 neurons in the hippocampus of anesthetized rats. *Hippocampus* 10:207–212.
- Martín-Vázquez G, Makarova J, Makarov VA, Herreras O (2013) Determining the true polarity and amplitude of synaptic currents

- underlying gamma oscillations of local field potentials. *PLoS ONE* 8(9):e75499.
- Martín-Vázquez G, Benito N, Makarov VA, Herreras O, Makarova J (2015) Diversity of LFPs activated in different target regions by a common CA3 input. *Cereb Cortex*. <http://dx.doi.org/10.1093/cercor/bhv211>. in press.
- Mazzucato L, Fontanini A, La Camera G (2015) Dynamics of multistable states during ongoing and evoked cortical activity. *J Neurosci* 35:8214–8231.
- Mitzdorf U, Singer W (1977) Laminar segregation of afferents to lateral geniculate nucleus of the cat: an analysis of current source density. *J Neurophysiol* 40:1227–1244.
- Murthy VN, Fetz EE (1996) Synchronization of neurons during local field potential oscillations in sensorimotor cortex of awake monkeys. *J Neurophysiol* 76:3968–3982.
- Niedermeyer E (2003) The clinical relevance of EEG interpretation. *Clin Electroencephalogr* 34:93–98.
- Nunez PL, Srinivasan R (2006) *Electric Fields in the Brain*. OUP: The Neurophysics of EEG.
- Onton J, Westerfield M, Townsend J, Makeig S (2006) Imaging human EEG dynamics using independent component analysis. *Neurosci Biobehav Rev* 30:808–822.
- Palva S, Palva JM (2007) New vistas for alpha-frequency band oscillations. *Trends Neurosci* 30:150–158.
- Pascual-Marqui RD, Biscay RJ, Bosch-Bayard J, Lehmann D, Kochi K, Kinoshita T, Yamada N, Sadato N (2014) Assessing direct paths of intracortical causal information flow of oscillatory activity with the isolated effective coherence (iCoh). *Front Hum Neurosci* 8:448.
- Pesaran B, Pezaris JS, Sahani M, Mitra PP, Andersen RA (2002) Temporal structure in neuronal activity during working memory in Macaque parietal cortex. *Nat Neurosci* 5:805–811.
- Petersen KH, Lindén H, Tetzlaff T, Einevoll GT (2014) Power laws from linear neuronal cable theory: power spectral densities of the soma potential, soma membrane current and single-neuron contribution to the EEG. *PLoS Comput Biol* 10(11):e1003928.
- Rall W (1967) Distinguishing Theoretical synaptic potentials computed for different soma-dendritic distributions of synaptic input. *J Neurophysiol* 30:1138–1168.
- Rall W, Shepherd GM (1968) Theoretical reconstruction of field potentials and dendrodendritic synaptic interactions in olfactory bulb. *J Neurophysiol* 31:884–915.
- Rasch M, Logothetis NK, Kreiman G (2009) From neurons to circuits: linear estimation of local field potentials. *J Neurosci* 29:13785–13796.
- Rauch A, Rainer G, Augath M, Oeltermann A, Logothetis NK (2008) Pharmacological MRI combined with electrophysiology in non-human primates: effects of Lidocaine on primary visual cortex. *Neuroimage* 40:590–600.
- Reimann MW, Anastassiou CA, Perin R, Hill SL, Markram H, Koch C (2013) A biophysically detailed model of neocortical local field potentials predicts the critical role of active membrane currents. *Neuron* 79:375–390.
- Rodríguez R, Haberly LB (1989) Analysis of synaptic events in the opossum piriform cortex with improved current source-density techniques. *J Neurophysiol* 61:702–718.
- Rudolph M, Pospischil M, Timofeev I, Destexhe A (2007) Inhibition determines membrane potential dynamics and controls action potential generation in awake and sleeping cat cortex. *J Neurosci* 27:5280–5290.
- Sakurai Y, Nakazono T, Ishino S, Terada S, Yamaguchi K, Takahashi S (2013) Diverse synchrony of firing reflects diverse cell-assembly coding in the prefrontal cortex. *J Physiol Paris* 107:459–470.
- Salami A, Eriksson J, Nyberg L (2012) Opposing effects of aging on large-scale brain systems for memory encoding and cognitive control. *J Neurosci* 32:10749–10757.
- Schomburg EW, Anastassiou CA, Buzsáki G, Koch C (2012) The spiking component of oscillatory extracellular potentials in the rat hippocampus. *J Neurosci* 32:11798–117811.
- Schomburg EW, Fernández-Ruiz A, Mizuseki K, Berényi A, Anastassiou CA, Koch C, Buzsáki G (2014) Theta phase segregation of input-specific gamma patterns in entorhinal-hippocampal networks. *Neuron* 84:470–485.
- Schönberger J, Draguhn A, Both M (2014) Lamina-specific contribution of glutamatergic and GABAergic potentials to hippocampal sharp wave-ripple complexes. *Front Neural Circuits* 8:103.
- Seyedhosseini M, Shushruth S, Davis T, Ichida JM, House PA, Greger B, Angelucci A, Tasdizen T (2015) Informative features of local field potential signals in primary visual cortex during natural image stimulation. *J Neurophysiol* 113:1520–1532.
- Softky WR, Koch C (1993) The highly irregular firing of cortical cells is inconsistent with temporal integration of random EPSPs. *J Neurosci* 13:334–350.
- Stevens CF, Zador AM (1998) Input synchrony and the irregular firing of cortical neurons. *Nat Neurosci* 1:210–217.
- Stone JV, Porrill J, Porter NR, Wilkinson ID (2002) Spatiotemporal independent component analysis of event-related fMRI data using skewed probability density functions. *Neuroimage* 15:407–421.
- Takehara-Nishiuchi K, McNaughton BL (2008) Spontaneous changes of neocortical code for associative memory during consolidation. *Science* 322:960–963.
- Turi G, Gotthardt S, Singer W, Vuong TA, Munk M, Wibral M (2012) Quantifying additive evoked contributions to the event-related potential. *Neuroimage* 59:2607–2624.
- Vanderwolf CH (1969) Hippocampal electrical activity and voluntary movement in the rat. *Electroencephalogr Clin Neurophysiol* 26:407–418.
- Varona P, Ibarz JM, López-Aguado L, Herreras O (2000) Macroscopic and subcellular factors shaping CA1 population spikes. *J Neurophysiol* 83:2192–2208.
- Vinogradova OS (1985) Expression, control, and probable functional significance of the neuronal theta-rhythm. *Prog Neurobiol* 45:523–583.
- Waldert S, Vigneswaran G, Philipp R, Lemon RN, Kraskov A (2015) Modulation of the intracortical LFP during action execution and observation. *J Neurosci* 35:8451–8461.
- Whitlock JR, Heynen AJ, Shuler MG, Bear MF (2006) Learning induces long-term potentiation in the hippocampus. *Science* 313:1093–1097.
- Willadt S, Nenniger M, Vogt KE (2013) Hippocampal feedforward inhibition focuses excitatory synaptic signals into distinct dendritic compartments. *PLoS One* 8(11):e80984.
- Womelsdorf T, Valiante TA, Sahin NT, Miller KJ, Tiesinga P (2014) Dynamic circuit motifs underlying rhythmic gain control, gating and integration. *Nat Neurosci* 17:1031–1039.
- Woodbury JW (1960) Potentials in a volume conductor. In: Ruch TC, Fulton JF, editors. *Medical Physiology and Biophysics*. Philadelphia and London: WB Saunders Co.. p. 83–91.

APPENDIX A. SUPPLEMENTARY DATA

Supplementary data associated with this article can be found, in the online version, at <http://dx.doi.org/10.1016/j.neuroscience.2015.09.054>.